Random Lasers With Coherent Feedback

Hui Cao, Junying Y. Xu, Yong Ling, Alexander L. Burin, Eric W. Seeling, Xiang Liu, and Robert P. H. Chang

Invited Paper

***Abstract*—We review our recent work on lasing in active random media. Light scattering, which had been regarded as detrimental to lasing action for a long time, actually provided coherent feedback for lasing. The fundamental difference and transition between a random laser with coherent feedback and a random laser with incoherent feedback were illustrated. We also trapped laser light in micrometer-sized random media. The trapping was caused by disorder-induced scattering and interference. This nontraditional way of light confinement has important applications to microlasers.**

***Index Terms*—Disordered system, optical scattering, random laser.**

I. Introduction

In 1966 LETOKHOV *et al*. invented a laser with nonresonant feedback using scattering reflector [1]. He further proposed a new way of generating light in a scattering medium with negative resonance [2]. In the 1980s, Markushev *et al.* observed lasing in Nd-doped laser crystal powder [3], [4]. They found a single particle, whose size is much larger than the optical wavelength, serves as a laser resonator. Since then, there has been much work on powder lasers [5]–[7]. In the early 1990s, Lawandy *et al*. reported stimulated emission from laser dye solution containing microparticles [8]. This observation triggered many experimental [9]–[14] and theoretical [15]–[18] studies on light amplification in diffusive media. The term "random laser" appeared. It represented a laser amplifier with feedback due to random scattering mechanism, as opposed to the reflective feedback by the mirrors. In this sense, the random laser is also called a mirrorless laser. However, the feedback provided by light scattering is incoherent, i.e., the feedback is basically intensity feedback. Thus, the physics is not dramatically different from the amplification of spontaneous emission (ASE) without feedback. In the late 1990s, random lasers with coherent feedback were realized with disordered semiconductor and organic materials [19]–[21]. The interference of backscattered waves produces the amplitude feedback.

In this paper, we review our recent experimental work on random lasers with coherent feedback. In Section II, we illustrate the difference between a random laser with incoherent feedback and a random laser with coherent feedback. Section III is focused on the coherent random laser. In Section VI, we describe the micro random laser. Section V contains the latest results on fabrication and characterization of a partially ordered random laser. We conclude in Section VI.

Manuscript received September 13, 2002; revised December 3, 2002. This work was supported in part by the National Science Foundation under the MRSEC program (DMR-0076097) at the Materials Research Center of Northwestern University. The work of H. Cao was supported by the David and Lucile Packard Foundation, and the Alfred P. Sloan Foundation.

The authors are with the Materials Research Center, Northwestern University, Evanston, IL 60208 USA (e-mail: h-cao@northwestern.edu).

Digital Object Identifier 10.1109/JSTQE.2002.807975

II. Two Types of Random Lasers

In an active random medium, light is scattered and undergoes a random walk before leaving the medium. Because of gain, a photon may induce the stimulated emission of a second photon as it travels in the medium. There are two characteristic length scales. One is the gain length, the distance a photon travels before generating a second photon. The other is the average path length that a photon travels in the gain medium. With an increase in the number of scattering centers, the average path length of photons in the medium increases. When it is equal to the gain length, on average every photon generates another photon before leaving the medium. The photon number increases with time. From the theoretical point of view, the solution to the diffusion equation including linear gain diverges [2]. This process has been called lasing with incoherent (nonresonant) feedback. It is similar to the neutron scattering in combination of nuclear fission.

When scattering gets stronger, after multiple scattering light may return to the scattering center from which it was scattered before, forming a closed-loop path for light. When the amplification along the loop reaches the loss, lasing oscillation occurs in the loop which serves as a cavity. The lasing frequency is determined by the requirement of constructive interference, i.e., the phase delay along the loop is equal to $2\pi m$, where m is an integer. Such a laser is called a random laser with coherent (resonant) feedback. Of course, the picture of a single closed-loop path for light is intuitive but naive. Light may return to its original position through many different paths. All the backscattered light interferes, and their phase relationship determines the lasing frequencies. Therefore, such random laser is a randomly distributed feedback laser. The feedback is provided by the disorder-induced scattering.

Experimentally, we observed the difference of the two types of random lasers and the transition between them [22]. The random medium used in our experiment is the rhodamine 640 dye solution containing ZnO nanoparticles. The dye serves as the gain medium and the nanoparticles are scattering centers. By varying the particle density in the solution, we continuously vary the amount of scattering. The frequency-doubled output ($\lambda = 532$ nm) of a mode-locked Nd:YAG laser (10-Hz repetition rate,

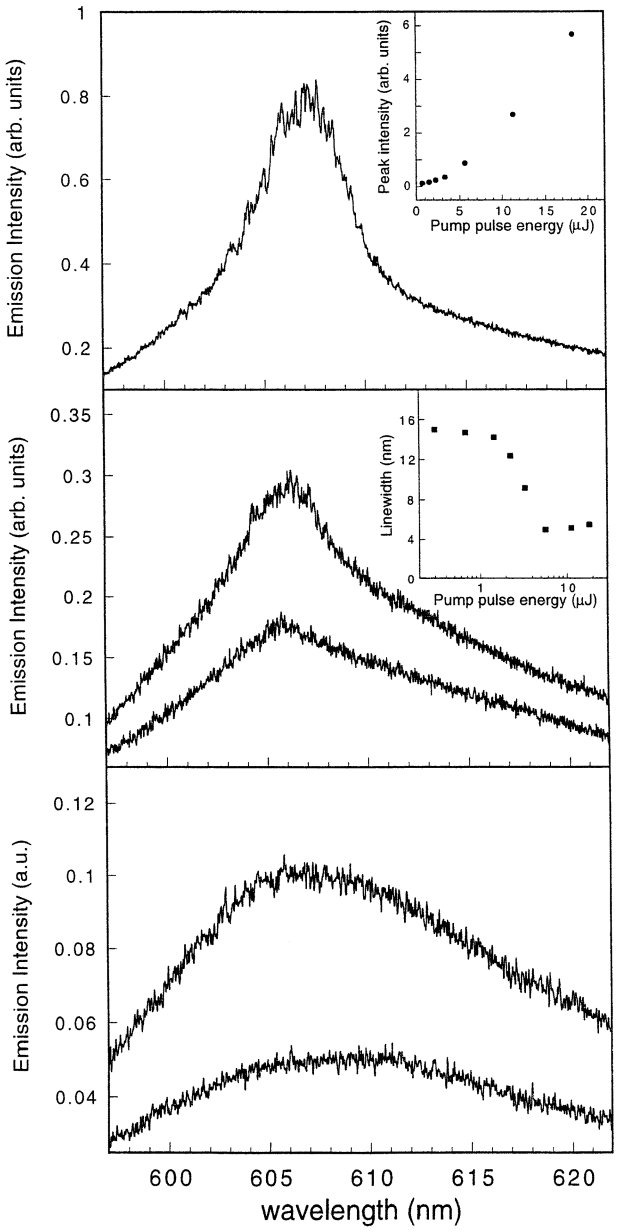

Fig. 1. Emission spectra when the incident pump-pulse energy is (from bottom to top) 0.68, 1.5, 2.3, 3.3, and 5.6 μJ. The ZnO particle density is $\sim 2.5 \times 10^{11}$ cm^{-3}. The upper inset is the emission intensity at the peak wavelength versus the pump-pulse energy. The lower inset is the emission linewidth versus the pump-pulse energy.

30-ps pulse width) was used to excite the dye molecules. We measured the single-shot emission spectrum using a 0.5-m spectrometer with a cooled charged-coupled device (CCD) detector array.

Fig. 1 shows the evolution of the emission spectra with the pump intensity when the ZnO particle density is $\sim 2.5 \times 10^{11}$ cm^{-3}. The dye concentration is fixed at 5×10^{-3} M. When the pump intensity reaches a threshold, a drastic spectral narrowing occurs. As shown in the insets of Fig. 1, when the incident pump-pulse energy exceeds ~ 3 μJ, the emission linewidth is quickly reduced to ~ 5 nm, meanwhile the peak emission intensity increases much more rapidly with the pump intensity. This is because optical scattering by the ZnO particles increases the path length of the emitted light inside the solution. Under optical pumping, the dye molecules have a broad gain spectrum. The gain length is shortest at the peak of the gain spectrum. As the pump intensity increases, the gain length decreases. When the shortest gain length becomes equal to the average length of light path in the gain volume, every photon generates a second photon by stimulated emission before leaving the solution. This triggered a "chain reaction," i.e., one photon generates two photons, and two photons generate four photons, etc. Thus, the photon density at the frequency of gain maximum builds up quickly. Away from the frequency of gain maximum, the gain length is still longer than the average path length of light in the solution. The chain reaction does not occur, and the photon density is still low. The drastic increase of photon density at the frequency of gain maximum results in an apparent narrowing of the emission spectrum. This process in nature is more like ASE than lasing oscillation. However, typical ASE exhibits a gradual spectral narrowing with excitation intensity, while in a random medium, spectral narrowing occurs suddenly above a threshold (the middle inset of Fig. 1). Namely, the ASE in random medium has a threshold. Above the threshold, the rate of photon generation by stimulated emission exceeds the photon loss rate. The photon density would diverge without gain saturation [14]. Thus, gain saturation plays an important role in the ASE above the threshold. Below the threshold, gain saturation can be neglected, similar to the case of typical ASE. Following the convention [2], the process of light amplification by simulated emission above the threshold is referred to as lasing with nonresonant feedback.

Next, we keep the same dye concentration and increase the ZnO particle density to 1×10^{12} cm^{-3}. Fig. 2 plots the evolution of the emission spectra with pump intensity. We can see that the phenomenon is very different in the case of strong scattering. When the incident pump-pulse energy exceeds 1.0 μJ, discrete peaks emerge in the emission spectrum. The linewidth of these peaks is less than 0.2 nm, which is more than 50 times smaller than the linewidth of the ASE below the threshold. When the pump intensity increases further, more sharp peaks appear. The emergence of discrete spectral peaks indicates the existence of spatial resonance for light. In the solution, such resonance is caused by recurrent light scattering of nanoparticles. In other words, the discrete peaks represent the resonant modes of random cavities formed by recurrent light scattering. When the optical gain is sufficiently high, lasing occurs in the modes of the random cavities. This is lasing with coherent feedback.

We also studied the transition from lasing with incoherent feedback to lasing with coherent feedback. Fig. 3 shows the evolution of the emission spectra with the pump intensity when the ZnO particle density is $\sim 5 \times 10^{11}$ cm^{-3}. As the pump intensity increases, a drastic spectral narrowing occurs first. Then at higher pump intensity, discrete narrow peaks emerge in the emission spectrum. Because the amount of scattering in the solution is between the previous two cases, there is some, but not large, probability of a photon scattered back to the original position. Hence, the loss of the random cavities formed by recurrent scattering is quite high. The pump intensity re-

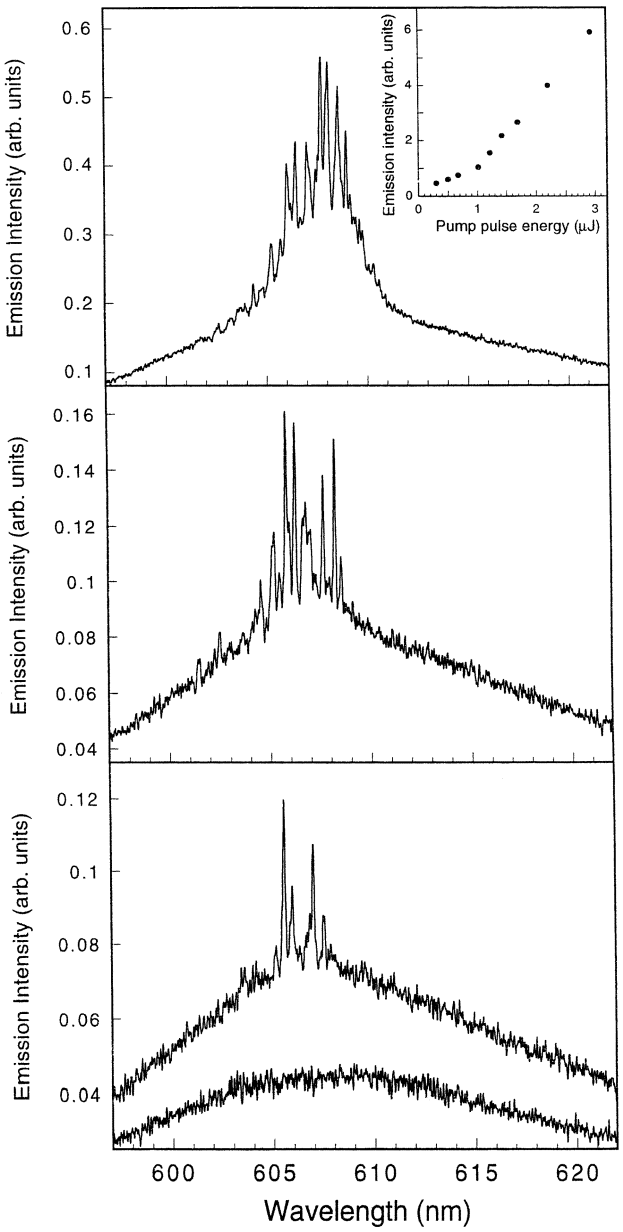

Fig. 2. Emission spectra when the incident pump-pulse energy is (from bottom to top) 0.68, 1.1, 1.3, and 2.9 μJ. The ZnO particle density is $\sim 1 \times 10^{12}$ cm^{-3}. The inset shows the emission intensity versus the pump-pulse energy.

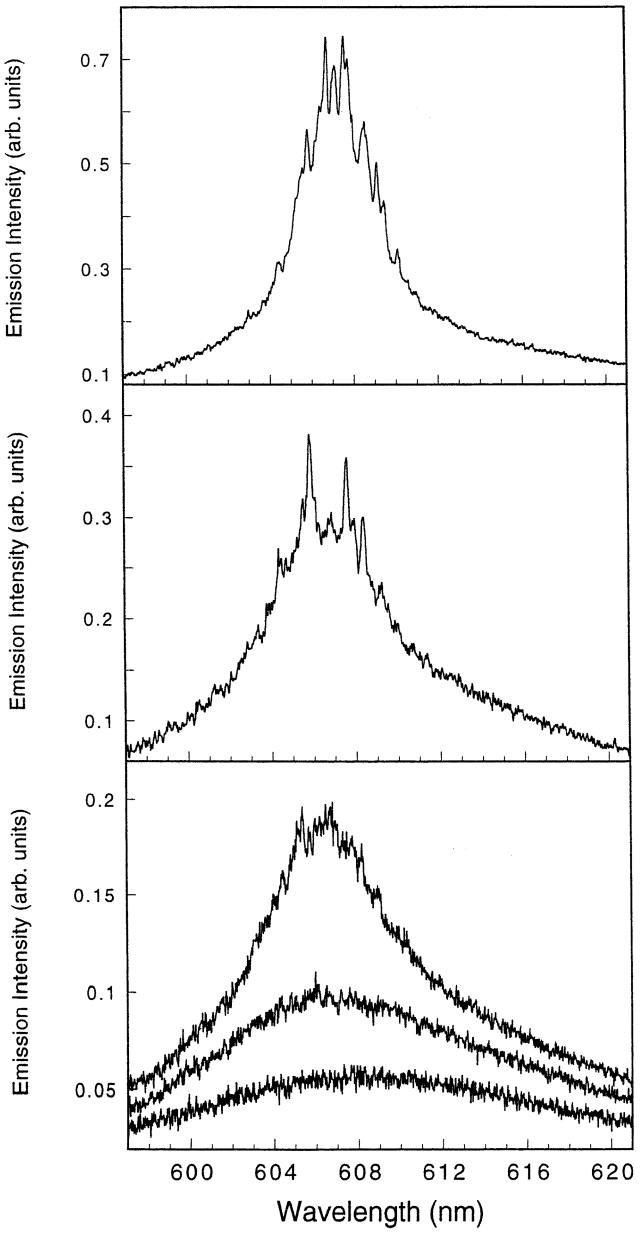

Fig. 3. Emission spectra when the incident pump-pulse energy is (from bottom to top) 0.74, 1.35, 1.7, 2.25, and 3.4 μJ. The ZnO particle density is $\sim 6 \times 10^{11}$ cm^{-3}.

quired to reach lasing threshold in these cavities is high. Thus, the pump intensity first reaches the threshold where the gain length at the peak of gain spectrum becomes equal to the average length of light path in the excitation volume. A significant spectral narrowing and a drastic increase of peak emission intensity occur, similar to what happens in Fig. 1. Then the pump intensity reaches a second threshold where the gain exceeds the loss in some random cavities. Lasing oscillation occurs in these cavities, adding discrete peaks to the emission spectrum. However, the number of lasing modes in Fig. 3 is less than that in Fig. 2 at similar pump intensity due to weaker scattering. Therefore, there exist two thresholds. The first threshold is for lasing with incoherent feedback, and the second is for lasing with coherent feedback.

From the viewpoint of ray optics, lasing with incoherent feedback is related to the instability of light amplification along open trajectories, while lasing with coherent feedback corresponds to the instability of light amplification along closed-loop paths. Therefore, the contribution of optical scattering to these two types of random lasers is very different. In the random laser with incoherent feedback, scattering merely increases the path length of light in the gain medium to reach the gain length. In the random laser with coherent feedback, scattering brings light back to its original position to interfere.

III. Random Laser With Coherent Feedback

There are three important length scales for the random laser: scattering length, gain length, and sample size. We studied the

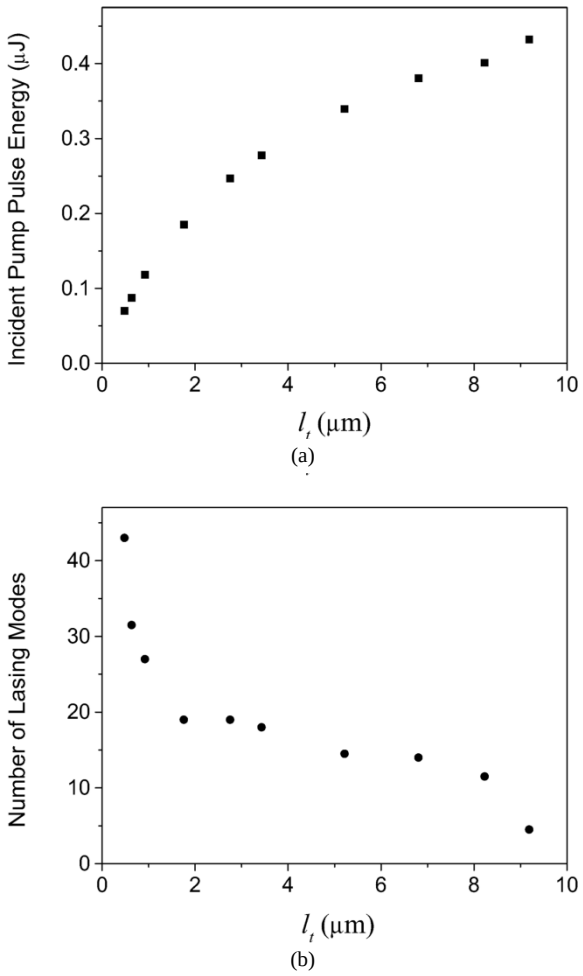

Fig. 4. (a) Incident pump-pulse energy at the lasing threshold versus the transport mean-free path l_t in the PMMA films. The dashed line is the fitted curve represented by $P_{\rm th} = 0.13 l_t^{0.53}$. (b) Number of lasing modes as a function of the transport mean-free path l_t in the PMMA sheets. The incident pump-pulse energy is 1.0 μJ.

dependence of lasing threshold on these parameters [23]. Next, we illustrate the essential role played by scattering in random laser with coherent feedback through its dependence on the scattering length.

The random media we used are polymethyl methacrylate (PMMA) sheets containing rhodamine 640 perchlorate dye and TiO_2 particles. The average diameter of TiO_2 particles is 400 nm. To change the scattering length, we varied the TiO_2 particle density in PMMA from 8×10^{10} to 6×10^{12} cm^{-3}. To characterize the transport mean-free path in these samples, we conducted a coherent backscattering experiment. The output from an He:Ne laser was used as the probe light, since its wavelength is very close to the emission wavelength of rhodamine 640 perchlorate dye. To avoid absorption of the probe light, we fabricated PMMA sheets which contains only TiO_2 particles but not the dye. From the angular width of the backscattering cone, we estimated the transport mean-free path l_t, after taking into account the internal reflection [24]. The detailed analysis of l_t can be found in [23].

The polymer samples were optically excited by the second harmonics of a pulsed Nd:YAG laser. The diameter of the pump spot at the sample surface is $\sim$50 μm. Fig. 4(a) plots the incident pump-pulse energy at the lasing threshold versus the transport mean-free path. The dye concentration in the polymer is fixed at 5×10^{-2} M. The lasing threshold decreases with the transport mean-free path. The strong dependence of the lasing threshold on the transport mean-free path clearly illustrates the important contribution of scattering to lasing. With an increase in the amount of optical scattering, the feedback provided by scattering becomes stronger. The random cavities formed by multiple scattering have lower loss. Hence, the lasing threshold is reduced. In Fig. 4(b), we plot the number of lasing modes in the samples with different mean-free path at the same pump intensity. With a decrease of the transport mean-free path, the number of lasing modes increases. This is because in a random medium with shorter mean-free path, there are more low-loss cavities formed by scattering. Hence, at the same pump intensity, lasing occurs in more cavities, leading to more lasing modes. An interesting feature in Fig. 4 is that when the transport mean-free path approaches the wavelength, the lasing threshold pump intensity drops quickly, and the number of lasing modes increases dramatically. Therefore, the regime $l_t \sim \lambda$ is important to both fundamental physics and practical application.

We realized random laser in the regime $l_t \sim \lambda$ with highly disordered semiconductor powder and polycrystalline films. We synthesized ZnO nanoparticles with the precipitation reaction [25]. The process involves hydrolysis of zinc salt in a polyol medium. ZnO nanoparticles are cold-pressed to form a pellet of thickness $\sim$1 mm. The average particle size is about 70 nm. The transport mean-free path was measured in the coherent back scattering experiment. ZnO has a direct band gap of 3.3 eV. To avoid absorption, the frequency-doubled output ($\lambda = 410$ nm) of a mode-locked Ti:Sapphire laser (76-MHz repetition rate, 200-fs pulse width) was used as the probe light. From the angle of the backscattering cone, we estimated $l_t \approx \lambda$.

The ZnO powder was optically pumped by the third harmonics ($\lambda = 355$ nm) of a mode-locked Nd:YAG laser (10-Hz repetition rate, 20-ps pulse width). The pump beam was focused to a 20-μm) spot on the sample surface. The emission spectrum was measured by a spectrometer with 0.13-nm spectral resolution. Simultaneously, the spatial distribution of the emitted light intensity in the powder was imaged by an ultraviolet (UV) microscope onto a UV sensitive CCD camera. The amplification of the microscope was about 100 times. The spatial resolution is $\sim$0.3 μm. A bandpass filter was placed in front of the microscope objective to block the pump light.

Fig. 5 shows the measured emission spectra and spatial distribution of emission intensity in ZnO powder at different pump intensities. At low pump intensity, the spectrum consists of a single broad spontaneous emission peak. Its full-width at half-maximum (FWHM) is $\sim$12 nm [Fig. 5(a)]. As shown in Fig. 5(b), the spatial distribution of the spontaneous emission intensity is smooth across the excitation area. Due to the pump intensity variation over the excitation spot, the spontaneous emission in the center of the excitation area is stronger. When the pump intensity exceeds a threshold, discrete narrow peaks emerge in the emission spectrum [Fig. 5(c)]. The FWHM of these peaks is less than 0.2 nm. Simultaneously, bright tiny spots appear in the near-field image of the emitted light distribution in the powder [Fig. 5(d)]. The size of the bright

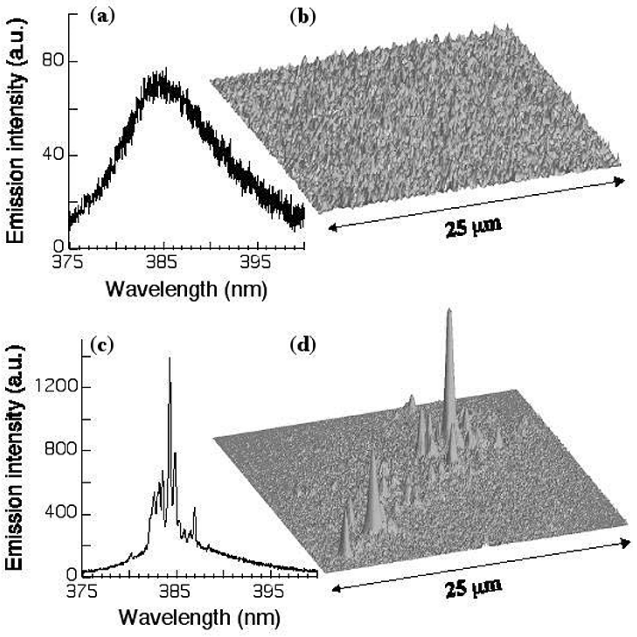

Fig. 5. (a) and (c) Measured spectra of emission from the ZnO powder. (b) and (d) Measured spatial distribution of emission intensity in the powder. The incident pump-pulse energy is 5.2 nJ for (a) and (c), and 12.5 nJ for (b) and (d).

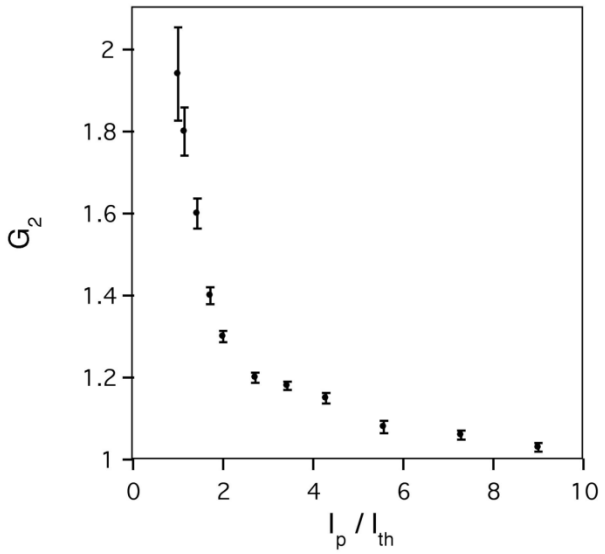

Fig. 6. Normalized second-order correlation coefficient G_2 as a function of the ratio of the incident pump intensity I_p to the threshold intensity $I_{\rm th}$.

spots at the sample surface is between 0.3 and 0.7μm. When the pump intensity is increased further, additional sharp peaks emerge in the emission spectrum. Correspondingly, more bright spots appear in the image of the emitted light distribution. The frequencies of the sharp peaks depend on the sample position. As we moved the excitation spot across the sample, the frequencies of the sharp peaks changed.

Above the threshold where discrete spectral peaks appear, the emission intensity increases much more rapidly with the pump intensity. Simultaneously, the emission pulse is shortened drastically from $\sim$200 ps below the threshold to less than 30 ps well above the threshold [26]. Our photocounting experiment reveals that the photon number distribution in a single mode changes continuously from the Bose–Einstein distribution at the threshold to Poisson distribution well above the threshold [27]. As shown in Fig. 6, the normalized second-order correlation coefficient G_2 decreases gradually from two to one when the pump intensity increases. This result indicates photon number fluctuation in each lasing mode is quenched by gain saturation well above the threshold. In contrast, for a random laser with incoherent feedback, the photon number distribution in a single mode remains Bose–Einstein distribution even well above the lasing threshold [28].

We investigated the dynamics of individual lasing modes in ZnO powder [26]. Lasing oscillation in different modes starts at different times, and it lasts for different periods of time. Their unsynchronized behavior suggests that these lasing modes originate from different cavities. As shown in Fig. 5(d), above the lasing threshold, the emission pattern exhibits spatially separated regions of intense laser radiation. Due to the local variation of particle density and spatial configuration, there exist small regions of stronger scattering. Light can be confined in these regions through the process of multiple scattering and interference. For a particular configuration of scatterers, only light at certain wavelengths can be confined, because the interference effect is wavelength sensitive. In a different part of the sample, the configuration of the scatterers is different, thus light at different wavelengths is confined. In other words, there are many small resonant cavities in the powder. In a finite-sized sample, the trapping of light is incomplete because photons can escape through the boundaries. This gives rise to the cavity loss. When the optical gain reaches the loss, lasing occurs in these cavities.

Unlike the conventional lasers with directional output, laser emission from the random media could be observed in all directions. The laser emission spectra vary with the observation angle. Since different random cavities have different output directions, lasing modes observed at different angles are different.

IV. Micro Random Laser

The results of Section III illustrate that the disorder-induced optical scattering not only provides coherent feedback for lasing, but also leads to spatial confinement of laser light in micrometer-sized volume. Utilizing this new mechanism of optical confinement, we fabricated microlasers with disordered media [29].

To fabricate micrometer-sized random medium, we agglomerated ZnO nanoparticles to form clusters whose size varies from half to a few micron [30]. The inset of Fig. 7 is the scanning electron microscope (SEM) image of a typical ZnO cluster. The size of the cluster is about 1.7 μm. It contains roughly 20 000 ZnO nanocrystallites. The ZnO cluster is optically pumped by the third harmonics of a pulsed Nd:YAG laser. The pump light is focused by a microscope objective onto a single cluster. We simultaneously measured the spectrum of emission from the cluster and imaged the spatial distribution of the emitted light intensity in the cluster.

At low pump intensity, the emission spectrum consists of a single broad spontaneous emission speak [Fig. 8(a)]. Its FWHM

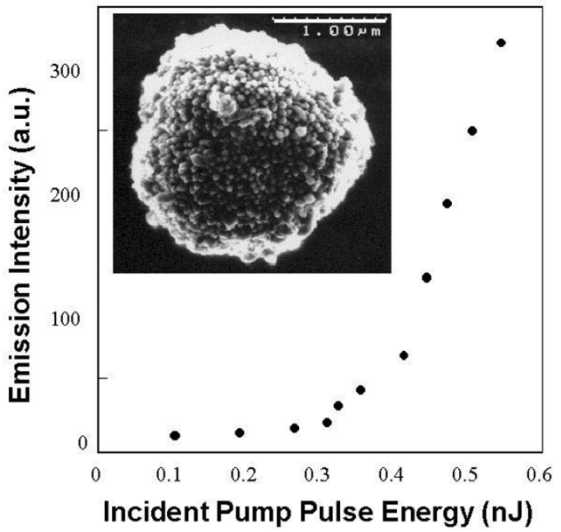

Fig. 7. Spectrally integrated intensity of emission from the ZnO cluster versus the incident pump-pulse energy. The inset is the SEM image of the ZnO cluster.

is 12 nm. The spatial distribution of the spontaneous emission intensity is uniform across the cluster [Fig. 8(b)]. When the pump intensity exceeds a threshold, a sharp peak emerges in the emission spectrum [Fig. 8(c)]. Its FWHM is 0.22 nm. Simultaneously, a couple of bright spots appear in the image of the emitted light distribution in the cluster [Fig. 8(d)]. When the pump intensity is increased further, a second sharp peak emerges in the emission spectrum [Fig. 8(e)]. Correspondingly, additional bright spots appear in the image of the emitted light distribution [Fig. 8(f)].

As shown in Fig. 7, above the pump intensity at which sharp spectral peaks and bright spots appear, the emission intensity increases almost linearly with the pump intensity. These data suggest that lasing occurs in the micrometer-sized cluster. The incident pump-pulse energy at the lasing threshold is $\sim$0.3 nJ. Note that less than 1% of the incident pump light is absorbed. The rest is scattered.

Since the cluster is very small, optical reflection from the boundary of the cluster might have some contribution to light confinement in the cluster. However, the laser cavity is not formed by total internal reflection at the boundary. Otherwise, the spatial pattern of laser light would be a bright ring near the edge of the cluster [31]. We believe the three-dimensional (3-D) optical confinement in a micrometer-sized ZnO cluster is achieved through disorder-induced scattering and interference. Since interference effect is wavelength sensitive, only light at certain wavelengths can be confined in the cluster. In another cluster of different particle configuration, light at different wavelengths is confined. Hence, the lasing frequencies are fingerprints of the clusters. Because optical confinement is not caused by light reflection at the surface of a cluster, but by scattering inside the cluster, we can achieve lasing in clusters with irregular shapes and rough surfaces.

We would like to compare the micro random laser with other types of microlasers. Over the past decade, several types of microlasers have been developed. The key issue for microlaser is to confine light in a small volume with dimensions on the

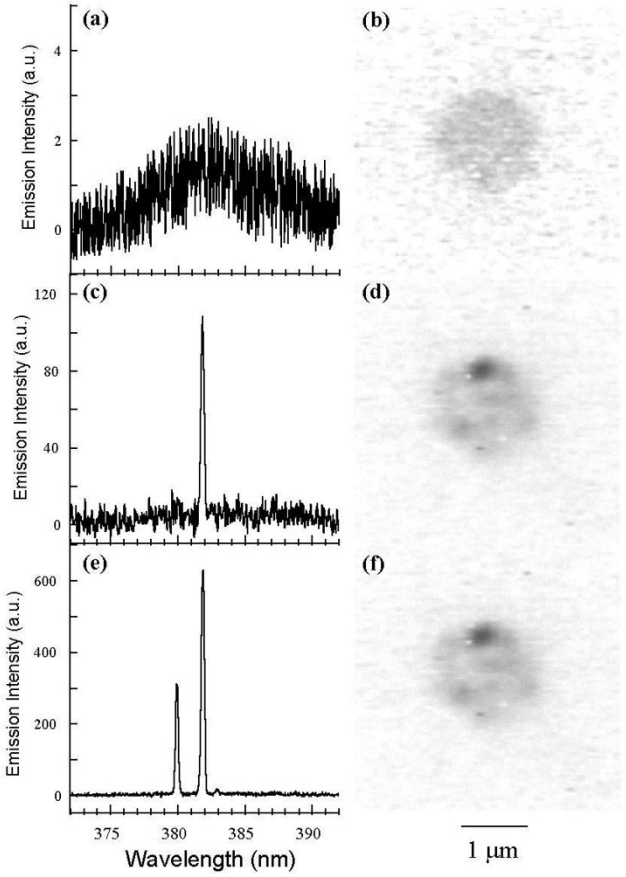

Fig. 8. (a), (c), and (e) Spectra of emission from the ZnO cluster shown in Fig. 7. (b), (d), and (f) Corresponding spatial distribution of emission intensity in the cluster. The incident pump-pulse energy is 0.26 nJ for (a) and (b), 0.35 nJ for (c) and (d), and 0.50 nJ for (e) and (f).

order of optical wavelength. In the vertical-cavity surface-emitting laser, light is confined by two distributed Bragg reflectors [32]. The microdisk laser utilizes total internal reflection at the edge of a high index disk to form whispering gallery modes [33]. In the two-dimensional (2-D) photonic band-gap defect mode laser, lateral confinement of light is realized through Bragg scattering in a 2-D periodic structure [34]. The fabrication of these microlasers requires expensive crystal growth and nanofabrication facilities. In micro random laser, the optical confinement is achieved through disorder-induced scattering and interference. The fabrication of the micro random laser is much easier and cheaper than that of most microlasers.

V. Partially Ordered Random Laser

Our latest numerical calculation shows that the threshold of a random laser can be reduced by incorporating some degree of order into an active random medium [35]. Recently, we developed a technique to synthesize monodisperse ZnO colloidal spheres and assemble them to form partially ordered structures [36].

Monodisperse ZnO colloidal spheres were produced by two-stage reaction process. In the primary reaction, polydisperse ZnO colloidal spheres were produced by hydrolysis of zinc acetate dihydrate (ZnAc). In the reaction, 0.03 mol ZnAc was

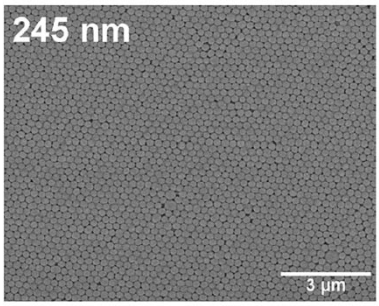

Fig. 9. SEM micrograph of monodisperse ZnO colloidal spheres in FCC array. The diameter of ZnO sphere is 245 nm.

added to 300-ml diethylene glycol (DEG). After the solution was heated to 160 °C, the precipitation of ZnO occurred. The reaction product was placed in a centrifuge to separate the ZnO particles from supernatant (DEG, dissolved reaction products, unreacted ZnAc, and water). The supernatant was decanted off and saved; the polydisperse ZnO particles were discarded. A secondary reaction was then performed in the same procedure as the primary reaction, except that prior to precipitation (typically at 150 °C) some amount of the purified primary reaction solution was added to the mixture. Following this addition, there was a temperature drop, and precipitation would typically occur at a lower temperature than that without such an addition. After reaching 160 °C, the reaction was stirred for one hour, after which the heat source was removed and the solution cooled to room temperature.

The SEM image in Fig. 9 shows that the ZnO synthesized with this technique consists of monodisperse colloidal spheres. Careful analysis of the micrographs reveals that the ZnO spheres are monodisperse within 5%–8%. The size of the spheres varies inversely and monotonically with the amount of primary solution added. Using this method, we synthesized monodisperse ZnO colloidal spheres over a broad size range (from 100 to 600 nm), with good control over the diameter. The high resolution transmission electron micrographs show that the spheres are made up of numerous nanocrystallites. X-ray diffraction analysis of the colloid reveals that the material is hexagonal ZnO with a crystallite size of 10–20 nm and no preferential growth direction.

To produce ordered array of ZnO colloidal spheres, they were sedimented directly from the reaction solution. While sedimentation at low temperature produced disordered structure, drying the solution on a substrate heated to 160 °C produced an ordered face center cubic (FCC) structure with domain size in excess of 10 μm (Fig. 9). For the ordered samples, photonic band gap (PBG) was observed in the normal-incidence transmission spectra of white light. The ratio of the center wavelength λ_c of the band gap to the sphere diameter d remains a constant (2.1) to within a few percent over all samples.

Since the ZnO colloidal sphere consist of numerous nanocrystallites, its density and refractive index differ from that of bulk ZnO. To obtain the effective refractive index of ZnO spheres, we calculated the PBG of 3-D FCC lattices of dielectric spheres with variable refractive index and diameter. By matching the measured ratio $\lambda_c/d \simeq 2.1$ to our calculation result, we found the effective refractive index of ZnO spheres $n_{\text{eff}} \simeq 1.6$. This value is smaller than the refractive index of bulk ZnO, confirming the ZnO colloidal spheres are porous.

We optically pumped the monodisperse ZnO colloidal spheres with the third harmonics of a pulsed Nd:YAG laser. Lasing occurred in both ordered and disordered arrays of ZnO spheres. The lasing threshold for the ordered array of ZnO spheres is lower than that for the disordered array of ZnO spheres. For the ordered arrays of monodisperse ZnO spheres with different diameters, the lasing threshold reaches the minimum when the PBG in (111) direction overlaps with the ZnO emission band. Full analysis is under way to interprete these results.

VI. Conclusion

We have reviewed our experimental studies of coherent random lasers. For a long time, light scattering had been regarded as detrimental to lasing action. We have shown that strong scattering can facilitate lasing by forming cavities and supplying coherent feedback. Our experimental results demonstrated that coherent light can be generated in a disordered medium with gain. We have illustrated the similarity and difference between a random laser and a conventional laser.

Disorder-induced scattering not only provides coherent feedback for lasing, but also leads to spatial confinement of laser light in micrometer-sized volume. Utilizing this new mechanism of optical confinement, we fabricated microlasers with disordered media.

Following the first demonstration of coherent random laser, there have been many experimental [37]–[42] and theoretical [43]–[50] studies of this nontraditional laser. The studies of random laser not only lead to advances in laser physics and light localization, but also improved our understanding of galaxy masers in which the feedback is also caused by scattering [51]

References

[1] R. V. Ambartsumian, N. G. Basov, P. G. Kryukov, and V. S. Letokhov, "Lasers with nonresonant feedback," *IEEE J. Quantum Electron.*, vol. QE-2, pp. 442–446, 1966.

[2] V. S. Letokhov, "Generation of light by a scattering medium with negative resonance absorption," *Sov. Phys.—JETP*, vol. 26, pp. 835–840, 1968.

[3] V. M. Markushev, V. F. Zolin, and C. M. Briskina, "Luminescence and stimulated emission of neodymium in sodium lanthanum molybdate powders," *Sov. J. Quantum Electron.*, vol. 16, pp. 281–283, 1986.

[4] V. M. Markushev, N. E. Ter-Gabrielyan, C. M. Briskina, V. R. Belan, and V. F. Zolin, "Stimulated emission kinetics of neodymium powder lasers," *Sov. J. Quantum Electron.*, vol. 20, pp. 773–777, 1990.

[5] C. Gouedard, D. Husson, C. Sauteret, F. Auzel, and A. Migus, "Generation of spatially incoherent short pulses in laser-pumped neodymium stoichiometric crystals and powders," *J. Opt. Soc. Amer. B*, vol. 10, pp. 2358–2363, 1993.

[6] M. A. Noginov, N. E. Noginova, H. J. Caulfield, P. Venkateswarlu, T. Thompson, M. Mahdi, and V. Ostroumov, "Short-pulsed stimulated emission in the powders of NdAl3(BO3)4, NdSc3(BO3)4, and Nd:Sr5(PO4)3F laser crystals," *J. Opt. Soc. Amer. B*, vol. 13, pp. 2024–2033, 1996.

[7] M. A. Noginov, S. U. Egarievwe, N. E. Noginova, H. J. Caulfield, and J. C. Wang, "Interferometric studies of coherence in a powder laser," *Opt. Mater.*, vol. 12, pp. 127–134, 1999.

[8] N. M. Lawandy, R. M. Balachandran, A. S. L. Gomes, and E. Sauvain, "Laser action in strongly scattering media," *Nature*, vol. 368, pp. 436–438, 1994.
[9] W. Sha, C.-H. Liu, and R. Alfano, "Spectral and temporal measurements of laser action of rhodamine 640 dye in strongly scattering media," *J. Opt. Soc. Amer. B*, vol. 19, pp. 1922–1924, 1994.
[10] M. A. Noginov, H. J. Caulfield, N. E. Noginova, and P. Venkateswarlu, "Line narrowing in the dye solution with scattering centers," *Opt. Commun.*, vol. 118, pp. 430–437, 1995.
[11] D. Zhang, B. Cheng, J. Yang, Y. Zhang, W. Hu, and Z. Li, "Narrow-bandwidth emission from a suspension of dye and scatterers," *Opt. Commun.*, vol. 118, pp. 462–465, 1995.
[12] M. Siddique, R. R. Alfano, G. A. Berger, M. Kempe, and A. Z. Genack, "Time-resolved studies of stimulated emission from colloidal dye solutions," *Opt. Lett.*, vol. 21, pp. 450–452, 1996.
[13] G. van Soest, M. Tomita, and A. Lagendijk, "Amplifying volume in scattering media," *Opt. Lett.*, vol. 24, pp. 306–308, 1999.
[14] G. van Soest, F. J. Poelwijk, R. Sprik, and A. Lagendijk, "Dynamics of a random laser above threshold," *Phys. Rev. Lett.*, vol. 86, pp. 1522–1525, 2001.
[15] S. John and G. Pang, "Theory of lasing in a multiple-scattering medium," *Phys. Rev. A*, vol. 54, pp. 3642–3652, 1996.
[16] D. S. Wiersma and A. Lagendijk, "Light diffusion with gain and random lasers," *Phys. Rev. Lett.*, vol. 54, pp. 4256–4265, 1996.
[17] R. M. Balachandran, N. M. Lawandy, and J. A. Moon, "Theory of laser action in scattering gain media," *Opt. Lett.*, vol. 22, pp. 319–321, 1997.
[18] G. A. Berger, M. Kempe, and A. Z. Genack, "Dynamics of stimulated emission from random media," *Phys. Rev. E*, vol. 56, pp. 6118–6122, 1997.
[19] H. Cao, Y. G. Zhao, H. C. Ong, S. T. Ho, J. Y. Dai, J. Y. Wu, and R. P. H. Chang, "Ultraviolet lasing in resonators formed by scattering in semiconductor polycrystalline films," *Appl. Phys. Lett.*, vol. 73, pp. 3656–3658, 1998.
[20] H. Cao, Y. Zhao, S. T. Ho, E. W. Seelig, Q. H. Wang, and R. P. H. Chang, "Random laser action in semiconductor powder," *Phys. Rev. Lett.*, vol. 82, pp. 2278–2281, 1999.
[21] S. V. Frolov, Z. V. Vardeny, K. Yoshino, A. Zakhidov, and R. H. Baughman, "Stimulated emission in high-gain organic media," *Phys. Rev. B*, vol. 59, pp. R5284–5287, 1999.
[22] H. Cao, J. Y. Xu, S.-H. Chang, and S. T. Ho, "Transition from amplified spontaneous emission to laser action in strongly scattering media," *Phys. Rev. E.*, vol. 61, pp. 1985–1989, 2000.
[23] Y. Ling, H. Cao, A. L. Burin, M. A. Ratner, X. Liu, and R. P. H. Chang, "Investigation of random lasers with resonant feedback," *Phys. Rev. A*, vol. 64, pp. 63 808–63 815, 2001.
[24] J. X. Zhu, D. J. Pine, and D. A. Weitz, "Internal reflection of diffusive light in random media," *Phys. Rev. A*, vol. 44, pp. 3948–3959, 1991.
[25] H. Cao, J. Y. Xu, D. Z. Zhang, S.-H. Chang, S. T. Ho, E. W. Seelig, X. Liu, and R. P. H. Chang, "Spatial confinement of laser light in active random media," *Phys. Rev. Lett.*, vol. 84, pp. 5584–5587, 2000.
[26] C. M. Soukoulis, X. Jiang, J. Y. Xu, and H. Cao, "Dynamic response and relaxation oscillation in random lasers," *Phys. Rev. B*, vol. 65, pp. R41103–41 106, 2002.
[27] H. Cao, Y. Ling, J. Y. Xu, C. Q. Cao, and P. Kumar, "Photon statistics of random lasers with resonant feedback," *Phys. Rev. Lett.*, vol. 86, pp. 4524–4527, 2001.
[28] R. V. Ambartsumyan, P. G. Kryukov, V. S. Letokhov, and Y. A. Matveets, "Statistical emission properties of a nonresonant feedback laser," *Sov. Phys.—JETP*, vol. 26, pp. 1109–1114, 1968.
[29] H. Cao, J. Y. Xu, E. W. Seelig, and R. P. H. Chang, "Microlasers made of disordered media," *Appl. Phys. Lett.*, vol. 76, pp. 2997–2999, 2000.
[30] D. Jezequel, J. Guenot, N. Jouini, and F. Fievet, "Submicrometer zinc oxide particles: Elaboration in polyol medium and morphological characteristics," *J. Mater. Res.*, vol. 10, pp. 77–83, 1995.
[31] H. Taniguchi, S. Tanosaki, K. Tsujita, and H. Inaba, "Experimental studies on output, spatial, and spectral characteristics of a microdroplet dye laser containing intralipid as a highly scattering medium," *IEEE J. Quantum Electron.*, vol. 32, pp. 1864–1864, Nov. 1996.
[32] J. L. Jewell, J. P. Harbison, A. Scherer, Y. H. Lee, and L. T. Florez, "Vertical-cavity surface-emitting lasers: Design, growth, fabrication, characterization," *IEEE J. Quantum Electron.*, vol. 27, pp. 1332–1346, June 1991.
[33] S. L. McCall, A. F. J. Levi, R. E. Slusher, S. J. Pearton, and R. A. Logan, "Whispering-gallery mode microdisk lasers," *Appl. Phys. Lett.*, vol. 60, pp. 289–291, 1992.
[34] O. Painter, R. K. Lee, A. Scherer, A. Yariv, J. D. O'Brien, P. D. Dapkus, and I. Kim, "Two-dimensional photonic band-gap defect mode laser," *Science*, vol. 284, pp. 1819–1821, 1999.
[35] A. Yamilov and H. Cao, "A Study of Random Laser Modes in Disordered Photonic Crystals," unpublished.
[36] E. W. Seelig, B. Tang, R. P. H. Chang, A. Yamilov, and H. Cao, "Self-Assembled 3-D Photonic Crystals From ZnO Colloidal Spheres," unpublished.
[37] R. K. Thareja and A. Mitra, "Random laser action in ZnO," *Appl. Phys. B*, vol. 71, pp. 181–184, 2000.
[38] R. C. Polson, A. Chipouline, and Z. V. Vardeny, "Random lasing in pi-conjugated films and infiltrated opals," *Adv. Mater. Process.*, vol. 13, pp. 760–764, 2001.
[39] G. Zacharakis, N. A. Papadogiannis, G. Filippidis, and T. G. Papazoglou, "Photon statistics of laserlike emission from polymeric scattering gain media," *Opt. Lett.*, vol. 25, pp. 923–925, 2001.
[40] G. R. Williams, S. B. Bayram, S. C. Rand, T. Hinklin, and R. M. Laine, "Laser action in strongly scattering rare-earth-metal-doped dielectric nanophosphors," *Phys. Rev. A*, vol. 65, pp. 13 807–13 812, 2001.
[41] D. S. Wiersma and S. Cavalier, "A temperature-tunable random laser," *Nature*, vol. 414, pp. 708–709, 2001.
[42] B. Li, G. Williams, S. C. Rand, T. Hinklin, and R. M. Laine, "Continuous-wave ultraviolet laser action in strongly scattering Nd-doped alumina," *Opt. Lett.*, vol. 27, pp. 394–396, 2002.
[43] X. Jiang and C. M. Soukoulis, "Time dependent theory for random lasers," *Phys. Rev. Lett.*, vol. 85, pp. 70–73, 2000.
[44] G. Hackenbroich, C. Viviescas, B. Elattari, and F. Haake, "Photocount statistics of chaotic lasers," *Phys. Rev. Lett.*, vol. 86, pp. 5262–5265, 2001.
[45] C. Vanneste and P. Sebbah, "Selective excitation of localized modes in active random media," *Phys. Rev. Lett.*, vol. 87, pp. 183 903–183 906, 2001.
[46] A. L. Burin, M. A. Ratner, H. Cao, and R. P. H. Chang, "Model for a random laser," *Phys. Rev. Lett.*, vol. 87, pp. 215 503–215 506, 2001.
[47] M. Patra, "Theory of photon statistics of random lasers," *Phys. Rev. A*, vol. 65, pp. 43 809–43 817, 2002.
[48] X. Jiang and C. M. Soukoulis, "Localized random lasing modes and a path for observing localization," *Phys. Rev. E*, vol. 65, pp. R25601–25 604, 2002.
[49] A. L. Burin, M. A. Ratner, H. Cao, and S.-H. Chang, "Random laser in one dimension," *Phys. Rev. Lett.*, vol. 88, pp. 93 904–93 907, 2002.
[50] V. M. Apalkov, M. E. Raikh, and B. Shapiro, "Random resonators and prelocalized modes in disordered dielectric films," *Phys. Rev. Lett.*, vol. 89, pp. 16 802–16 805, 2002.
[51] V. S. Letokhov, "Cosmic maser with feedback," *Sov. Astron.*, vol. 16, pp. 604–609, 1973.

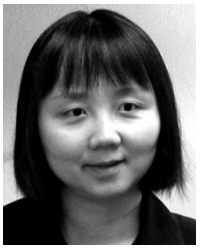

Hui Cao received the Ph.D. degree in applied physics from Stanford University, Stanford, CA, in 1997.

She is an Associate Professor in the Department of Physics and Astronomy at Northwestern University, Evanston, IL.

Dr. Cao won the David and Lucille Packard Fellowship, the Alfred P. Sloan Fellowship, and the NSF Early CAREER award.

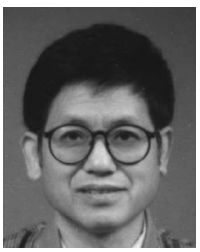

Junying Y. Xu graduated from the Physics Department of Nankai University, Tianjin, China in 1963.

From 1963 to 1998, he worked at the Semiconductor Institute of Chinese Academy of Sciences in Beijing, China, and engaged in the R & D of semiconductor optoelectronics devices. From 1998 to 2002, he was a Visiting Scholar at the Department of Physics and Astronomy, Northwestern University, Evanston, IL.

Yong Ling received the B.S., M.S., and Ph.D. degrees from the Department of Physics, Tsinghua University, China, in 1985, 1988, and 1996, respectively.

From 1999 to 2001, he worked as a Research Associate in the Department of Physics and Astronomy, Northwestern University, Evanston, IL. He has been an Associate Professor in the Department of Physics, Tsinghua University, since 1998. His current research focuses on analysis and fabrication of nano-materials and nano-structure.

Alexander L. Burin received the Ph.D. degree in condensed matter from Moscow Institute for Physics and Engineering, Moscow, Russia, in 1989.

He is a Research Associate in the Department of Chemistry and the Department of Physics and Astronomy at Northwestern University, Evanston, IL.

Eric W. Seeling received the B.S. degree in materials science from the Massachusetts Institute of Technology, Cambridge, in 1996. He is a graduate student in the Department of Materials Science and Engineering at Northwestern University, Evanston, IL.

His research has focused on developing methods for the production of ZnO used in the study of random lasers. More recently, he has developed a technique for the production of monodisperse ZnO colloidal spheres for the study of both random lasing and optically active self-assembled photonic crystals.

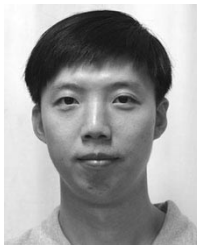

Xiang Liu received the B.E. degree in materials science and engineering from Tsinghua University, China, in 1996. He is a Ph.D. student in the Department of Materials Science and Engineering, Northwestern University, Evanston, IL.

Robert P. H. Chang received the S.B. degree in physics from the Massachusetts Institute of Technology, Cambridge, and the Ph.D. degree in astrophysics from Princeton University, Princeton, NJ.

He served as a Technical Staff Member in the Research Division of Bell Labs for 15 years. He is currently Director of the Materials Research Center and Materials Research Institute at Northwestern University, Evanston, IL. Since 1986, he has also served as Professor of Materials Science and Engineering and Professor of Electrical and Computer Engineering. An active contributor to scientific literature, he has had more than 200 papers published in international journals. Since 1994, he has served as Principal Editor of the *Journal of Materials Research* and an Advisory Board Member of the *Materials Chemistry and Physics Journal*. He has frequently been the recipient of invitations to provide keynote and plenary lectures at international meetings, as well as at other scientific institutions.

Dr. Chang is very active in the promotion of materials research internationally, being the First and Founding President of the International Union of Materials Research Societies (IUMRS). He is currently the General Chairman of the IUMRS. His honors include Member of the Materials Education Council, Chairman of the Advisory committee to Materials Research Laboratory at ITRI, and election to the rank of Fellow of the American Vacuum Society.